In asthma positive phase III slopes can result from structural heterogeneity of the bronchial tree

Verbanck, Sylvia A B; Foy, Brody Harry

Published in:
Journal of Applied Physiology (Bethesda, Md. : 1985)

DOI:
10.1152/japplphysiol.00687.2021

Publication date:
2022

License:
Unspecified

Document Version:
Accepted author manuscript

In asthma positive phase III slopes result from structural heterogeneity of the bronchial tree

Sylvia Verbanck *[1] and Brody H Foy [2,3]

[1] Respiratory Division, University Hospital (UZ Brussel), Vrije Universiteit Brussel (VUB), Brussels, Belgium.
[2] Center for Systems Biology and Dept of Pathology, Massachusetts General Hospital, Boston, MA, USA.
[3] Dept of Systems Biology, Harvard Medical School, Boston, MA, USA.

***Corresponding author:** Sylvia Verbanck
Respiratory Division
University Hospital (UZBrussel)
Laarbeeklaan 101
1090 Brussels, Belgium.

Author contributions: SV and BF contributed equally to study design, computational simulation and data analysis, interpretation of findings and manuscript writing.

Funding: This project was supported by the Fund for Scientific Research-Flanders (FWO-Vlaanderen, Belgium).

Running head: Structure-function link in asthma.

Word count (manuscript): 3819.

KEY WORDS: Ventilation heterogeneity, phase III slope, asthma, structure-function, computational lung model.

ABSTRACT

We have previously identified bronchial generations 5-7 as the locus of maximum contribution to the convective portion of the phase III slope in CT-based lung models of asthma patients. In the present study, we examined how phase III slope is generated locally, by specifically interrogating at individual branch points, the necessary condition for a phase III slope to occur: some degree of convective flow sequencing between any two daughter branches that have a heterogeneity in gas washout concentration between them. Flow sequencing at individual branch points showed a wide range of values, including branch points where flow sequencing was such that phase III slopes were negative locally. Yet, the net effect in the 24 bronchial trees that we studied was that flow sequencing between pairs of less and better ventilated units most frequently drove positive phase III slopes in generations 5-7. By investigating the link of local flow sequencing between any two daughter branches to the corresponding heterogeneity of mechanical lung properties, heterogeneity of compliance was seen to be a major determinant of flow sequencing. In these bronchial structures, compliance heterogeneity was essentially brought about by volume asymmetry resulting from terminating pathways within the 3D confines of the lung contours. We conclude that the serial and parallel combination of lung mechanical properties at individual branch points in an asymmetrical branching network generates flow sequencing in mid-range conductive airways, leading to a positive at-mouth phase III slope.

NEW AND NOTEWORTHY

Conceptually, the simplest way to obtain a sloping phase III during a washout exhalation is when there is convective flow sequencing between two lung units, such that the better ventilated unit contributes relatively more to exhaled flow at the beginning of phase III in the exhalation. Here, we show how compliance heterogeneity across the serial and parallel arrangement of branch points in bronchial trees of asthma patients leads to flow sequencing, and thus phase III slopes of positive sign at the patient's mouth.

INTRODUCTION

Convective ventilation heterogeneity plays an important role in healthy and diseased lungs and can refer to any difference in inspired gas concentration between lung units supplied by convection-dominated gas transport. Under normal breathing conditions in the adult human lung, this corresponds to the conductive airways of the tracheobronchial tree.[1] Resulting gas concentration heterogeneities would likely be visible at the resolution of various ventilation imaging modalities[2–4], where they are usually reported as 2D or 3D maps of specific ventilation. Even if these convection-dependent lung units with different specific ventilations empty in perfect synchrony, an at-mouth multiple breath N_2 washout curve would follow a multi-exponential decay.[5] Within each breath, a so-called N_2 phase III slope will only occur if in addition to this difference in specific ventilation, the lung units empty asynchronously, due to a flow sequencing pattern between them.[1]

We have recently simulated the convection-dependent portion of the phase III slope, reflected in the index of conductive lung zone heterogeneity (Scond), in realistic CT based bronchial structures of 24 asthma patients, using an experimentally and clinically validated mathematical model.[6] By examining the individual branch phase III slopes generated throughout the bronchial trees, we were able to identify bronchial generations 5-7 as the major source of Scond. In these bronchial airway generations, a difference in gas concentration becomes visible as a positive phase III slope (and positive Scond value) at the mouth, due to the significant asynchrony between the most and least ventilation lung units. By contrast, airway generations 2-4 also showed differences in gas concentration but these did not translate into a positive phase III slope at the mouth, because the above-described flow asynchrony was absent. Also noteworthy is that across the asthma patients under study, the wide range in phase III slope values could be reproduced solely based on the patient's CT-derived airway structure and functional residual capacity, and without any parameter fitting to artificially create flow sequencing.[7] Flow sequencing simply manifested itself because of basic mechanical properties such as the resistance and compliance dictated by each patient's airway morphology.

The raises a question: which structural features drive this specific asynchronous flow sequencing pattern? Given these asthma patients exhibited widely varying degrees of Scond elevation[6], further analysis of this cohort will enable us to scrutinize this structure-function link. The two obvious potential candidate structural features are heterogeneity of resistance and heterogeneity of compliance distributed across the tracheobronchial structure. Within this study we aimed to test these potential explanations and identify the source of structural heterogeneity inside the lungs that translates into convective ventilation heterogeneity visible at the mouth.

MATERIALS AND METHODS

The computational models used to simulate the multiple breath washout have been extensively described in prior work.[7–9] In brief, 24 asthmatic patients underwent inspiratory CT imaging (at total lung capacity) in supine position using a Sensation 16 scanner (Siemens,Forchheim,Germany), after receiving a bronchodilatory therapy (2.5mg nebulized salbutamol). From these scans, lobar and lung segmentation was performed, and centerlines and lumen cross sections of the large and middle airways (to an average generation 6-10) were extracted.[10] From the CT-extracted centerlines, an energy minimization algorithm was used to grow the remainder of the conducting airways, within the confines of the lobar boundaries (to an average generation of 16). The bronchial generations of interest (up to generation 7) where potential sources of flow sequencing are sought, concern in major part CT visible airways (in generation 7, 85% [IQR:82-90%] of airways are CT-extracted). The algorithmically generated space-filling airways then led to an average of 30,000 terminal branches (min: 17175, max: 45637), subtended by simple spherical volume units. All units had the same compliance, but the local pressure in the pleural cavity was assumed to vary linearly in the gravitational axis (using the same parameters for a 1L tidal volume as in prior work[7]). In the absence of other structural heterogeneity, this leads to gravitational variation in specific ventilation of each acinus, but a consistent pressure-volume curve for all acini. Median[IQR] total lung resistance of the 24 structures was 0.30 [0.24-0.49] kPa.s/L, which is concordant with prior reported lung resistance values.[11] For each of the 24 structures, multiple-breath washouts were simulated using a prior published mathematical model of ventilation and gas transport[9], and were

validated[7] using each patient's washout-estimated Scond, derived from the baseline data of a prior clinical study[12].

We quantified the degree of expiratory flow sequencing at every single branch point *(seq[flow]$_i$)*, across the 24 structures, identifying where local positive phase III slopes could arise at all. The flow sequencing at each branch point was defined as the difference in the percentage of flow contributed by each daughter airway to its parent flow from beginning to end of phase III (i.e., *seq[flow]*=0% corresponding to both daughters contributing in the same proportion to total flow at beginning and at end of phase III). Daughter branches were sorted such that the first daughter branch (d_1) was always the one with the lower washout concentration (resulting from the gas transport simulations in each structure). As a result, the value of *seq[flow]* at any given branch point needed to be positive in order to result in a positive N_2 phase III slope in the associated parent branch.

We quantified compliance heterogeneity ΔC at any branch *i*, as the relative difference between effective compliance of its two daughter branches

$$\Delta C_i = \frac{C_{d_1} - C_{d_2}}{\frac{1}{2}\left(C_{d_1} + C_{d_2}\right)}, \qquad (1)$$

where d_1 and d_2 denote the daughters of parent branch *i* (and d_1 is the daughter branch with the lower washout concentration) and where the effective compliance (*C*) of a branch is the summation of serial and parallel compliances of all subtending branches and spherical volume units. Each subtended volume unit had a constant compliance of $\frac{0.2}{N}$ L/cmH_2O, where N is the total number of volume units in the structure. In a similar process to equation (1), resistance heterogeneity (ΔR) was calculated as

$$\Delta R_i = \frac{R_{d_1} - R_{d_2}}{\frac{1}{2}\left(R_{d_1} + R_{d_2}\right)}, \qquad (2)$$

where the effective resistance (*R)* is calculated as the summation of serial and parallel resistances of the subtending branches (and d_1 is the daughter branch with the lower washout concentration), and where resistance of an individual branch (*Rb*) was approximated using a Pedley model[13]

$$Rb = \frac{32\mu Lc}{\pi d^4}\left(Re(Q)\frac{d}{L}\right)^{1/2} \qquad (3)$$

where *d* and *L* are branch diameter and length, μ is air viscosity, c = 1.85 is a correction constant, *Q* is the airflow rate in the branch, and *Re(Q)* is the Reynold's number of the air flow.

Finally, we calculated volume asymmetry of a branch *i* in three ways. First, this was done by considering heterogeneity of Horsfield order ($\Delta Horsf_i$) and of subtended volume (ΔV_i) exactly in the same way as was done for compliance and resistance heterogeneity (ΔC_i and ΔR_i) and thus calculated as

$$\Delta\text{Horsf}_i = Horsf_{d_1} - Horsf_{d_2} \qquad (4)$$

where $Horsf_{d_1}$and $Horsf_{d_2}$ are the Horsfield orders of the first and second daughter branches respectively, and

$$\Delta V_i = \frac{V_{d_1} - V_{d_2}}{\frac{1}{2}(V_{d_1} + V_{d_2})}, \qquad (5)$$

where $V_{d_1}$and V_{d_2} are the total lung volumes subtended by the first and second daughter branches respectively. Alternatively, an index of volumetric asymmetry VolAsym_i, which only accounts for structure (without any sorting on d_1 and d_2) was defined as

$$VolAsym_i = 1 - \frac{\min(V_{d_1}, V_{d_2})}{\max(V_{d_1}, V_{d_2})}, \qquad (6)$$

$VolAsym_i$ is defined to always be between 0 and 1, with higher numbers indicating greater asymmetry.

When calculating averages of $\Delta C, \Delta R, \Delta Horsf, \Delta V$ or *VolAsym* over a given bronchial generation or lung structure, each branch contribution was weighted by the ratio of its expiratory flow to total expiratory flow at the trachea. This weighted average was used to avoid excessive influence from units which only marginally contribute to overall ventilation. Of note, by definition, *VolAsym* and the coefficient of variation of washout gas concentration (*CoV(conc)*) are always positive, while

$\Delta C, \Delta R, \Delta Horsf, \Delta V$ and *seq[flow]* can be both positive and negative. For a given branch *i*, a positive $seq[flow]_i$ indicates that the branch with the lower washout gas concentration is the one emptying first (i.e., contributing relatively more to total flow at begin versus end of phase III and thus generating a positive phase III slope). A positive ΔC indicates that the branch with the lower washout gas concentration subtends the lung cul-de-sac with the greater compliance (i.e. $C_{d_1} > C_{d_2}$), and a negative ΔR indicates that the branch with the lower washout gas concentration has the lower effective resistance ($R_{d_1} < R_{d_2}$). If d_2 is the daughter branch furthest away from the terminal units, $\Delta \mathrm{Horsf}_i$ will be negative, and if d_2 subtends the largest cul-de-sac volume ΔV_i will be negative.

RESULTS

In **Figure 1**, we show concentration heterogeneity and flow sequencing against bronchial generation, stratified by the magnitude of their Scond values. Higher Scond values were associated with elevated concentration heterogeneity, in line with prior findings.[6] More importantly, a positive *seq[flow]* value – the necessary condition for a positive phase III slope at the mouth – predominantly occurs in generations 5 onwards and is not related to Scond magnitude (**Figure 1B**).

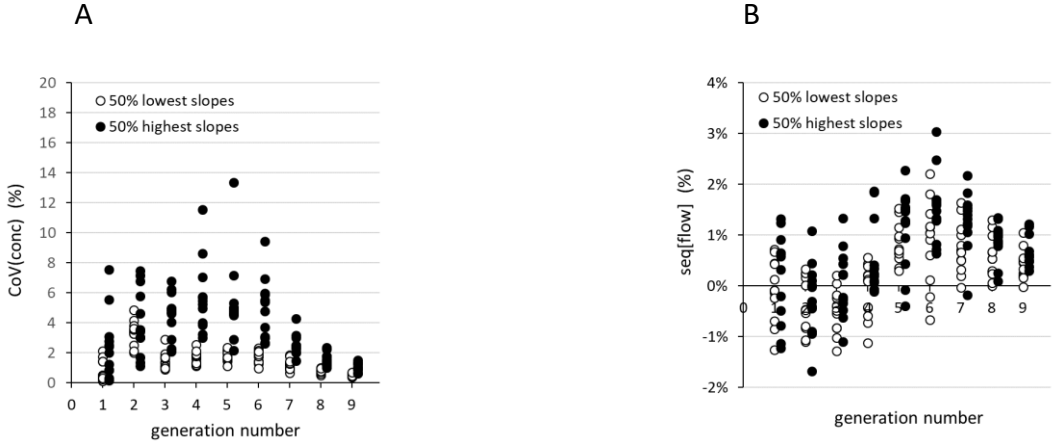

Figure 1 : Generation-averaged coefficient of variation of washout gas concentration (*CoV(conc)*) and flow sequence (*seq[flow]*) between any parallel pair of lung units as a function of airway generation number for all 24 lung structures, stratified according to patients' overall Scond value at the mouth (open circles : below median Scond; closed circles : at or above median Scond). While a non-zero CoV is present in most generations, a consistently positive *seq[flow*] value only exists in generations 5-9.

A different way to illustrate the degree of flow sequencing peaking in generation 6 (as shown in **Figure 1B**), is to plot airflow rates for all daughter pairs against each other, at a given generation, in a given asthmatic patient, normalized by each daughter's maximum flow rate (**Figure 2**). If the flow rates of two daughters are perfectly synchronous, they would move along the line of identity from -100% to 100% and back, while high degrees of asynchrony would generate curvilinear movement patterns. Results in **Figure 2** illustrate that for a given representative patient structure, flow asynchrony is most pronounced at generation 6.

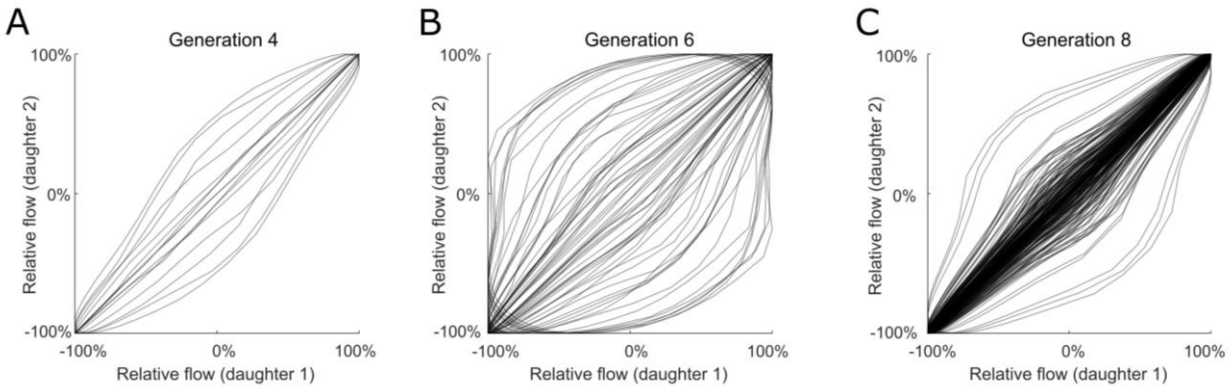

Figure 2: Relative airflow profiles throughout inhalation and exhalation for each pair of daughters to parents at branch generations 4, 6, and 8, for a representative asthmatic lung structure. Movement back and forth along the identify line represents no asynchrony, while higher curvature indicates higher asynchrony. Considerable flow asynchrony is seen to develop in generation 6, and less so in two generations up or down.

To illustrate how flow sequencing can arise in a simpler setting, we use a toy system comprising 4 generations and 11 branches (**Figure 3**). The primary branch had a radius of 1cm, and length of 10cm, with each subsequent generation having radius and length reduced by 60%. In the baseline case (case A), flow sequencing occurs only at 2 of the 5 branch points, namely where there is an asymmetry in arrangement of the terminal compliant units. In the other cases (B-D), the degree of flow sequencing gets modulated by the compliance of the terminal units itself (case B) or resistance of the airways (be it via length or radius; case C and D). These simple simulations show that asymmetrical structures due to uneven arrangement of compliant units produce flow asynchrony, and that magnitude of the flow asynchrony is modulated by terminal unit compliance and airway resistance.

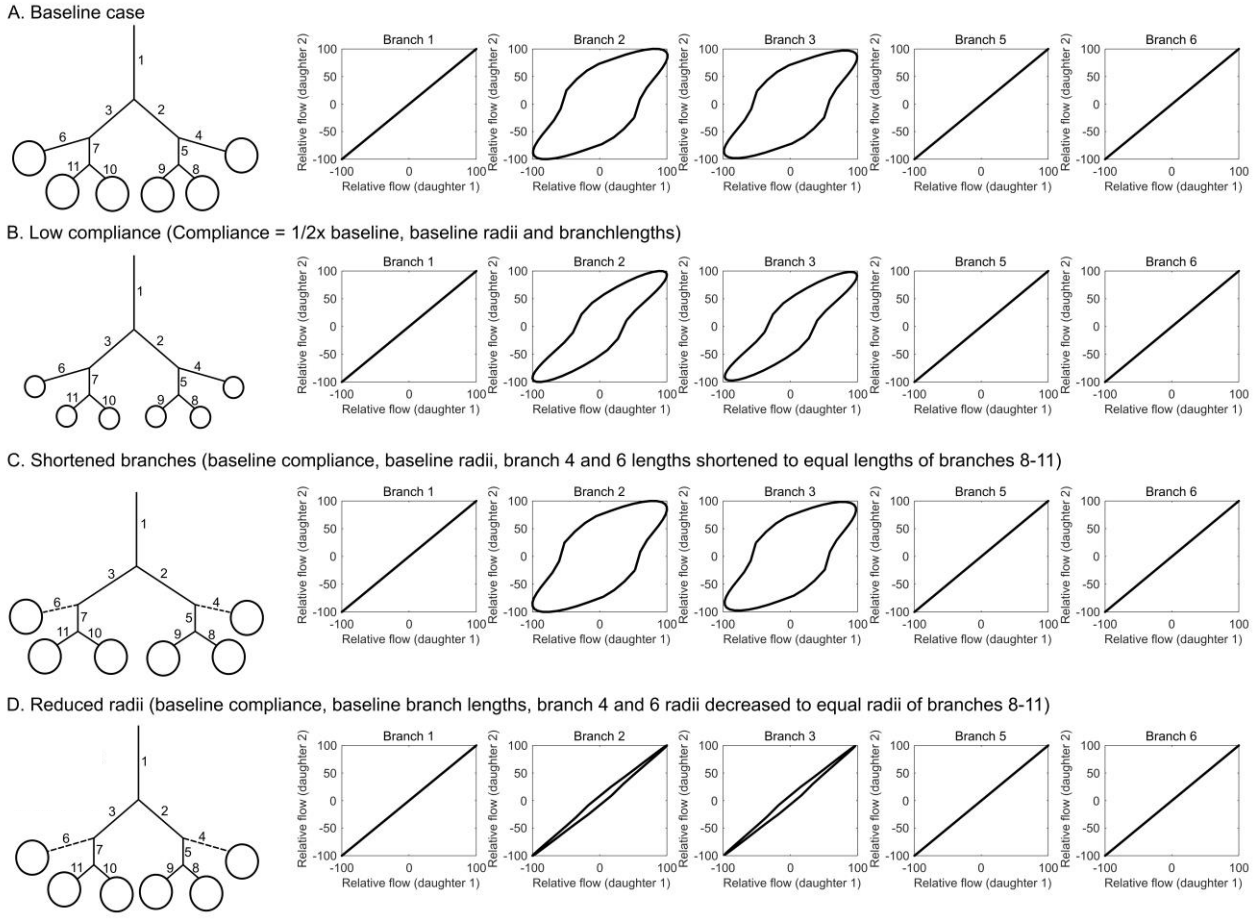

Figure 3: Relative airflow profiles throughout inhalation and exhalation for each pair of daughters to parents, with flow sequence developing at branches 2 and 3, but not at the other more peripheral or proximal branch points where the subtended structures are symmetrical (branch 1, 5 or 6).

For the complex realistic bronchial structures, **Figure 4** shows relationships between branch generation and flow sequencing, compliance heterogeneity, and resistance heterogeneity by compiling data from all 24 structures. The pattern of flow sequencing with a maximum in generations 5-7 (grey area) is mimicked by compliance heterogeneity, in that these generations carry a majority of branch points with a negative compliance difference (ΔC) between them. By attributing the first unit as the one with the lower inhaled concentration, the negative ΔC in these bronchial generations means that there is a majority of airway pairs for which airway daughter branches with the lower washout gas concentration subtends the cul-de-sac with the lower compliance compared to its sister branch (**Figure 4B**). Resistance heterogeneity (**Figure 4C**) does not show a consistent behavior in bronchial generations 5-7 in terms of its sign.

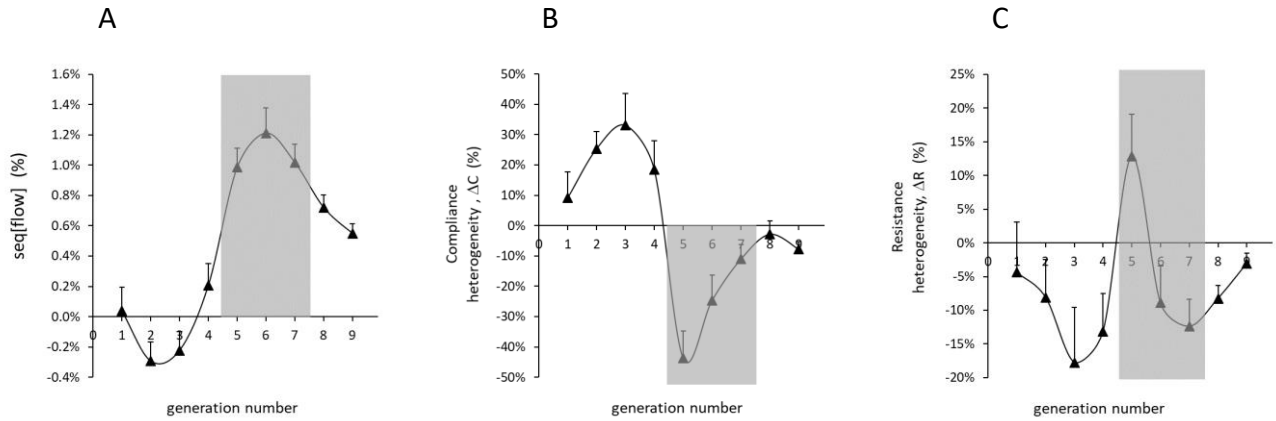

Figure 4: Generation-specific flow sequence (*seq[flow]*), heterogeneity of compliance (*ΔC*) and heterogeneity of resistance (*ΔR*) as a function of airway generation number; data obtained from all 24 lung structures is presented as means±SE; grey area indicates the generation range responsible for maximal phase-III slope contribution.[6] For a positive slope to occur at the mouth, *seq[flow]* needs to be positive; using the same convention that daughter branch d_1 is the one with the lower washout concentration, corresponding compliance and resistance heterogeneity (equations 1 and 2) are shown in the same representation.

To better characterize the determinant structural features of the daughter branches that subtend the better ventilated units in those generations where flow sequencing (positive *seq[flow]*) occurs, **Figure 5** shows corresponding heterogeneity of Horsfield order (**Figure 5A**) and of subtended volume (**Figure 5B**). While the latter closely mimics the pattern displayed by compliance heterogeneity (**Figure 4B**), both panels of **Figure 5** show that from 5 onwards the best ventilated units are the smaller and shorter ones, with a difference in Horsfield order between daughter branches peaking at 1.5 in generation 5.

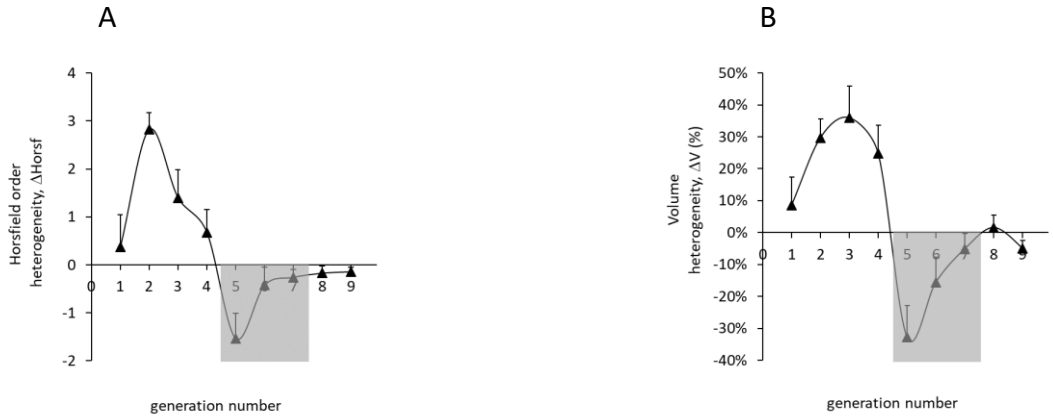

Figure 5: Generation-specific heterogeneity of Horsfield order (*ΔHorsf*) and heterogeneity of subtended volume (*ΔV*) as a function of airway generation number; same representation as Figure 4.

In **Figure 6** we present similar results for concentration heterogeneity (*CoV(conc)*) and a measure of structural asymmetry in terms of simple volume asymmetry (*VolAsym*). There is a significant degree of both volume and concentration asymmetry in the most proximal generations (**Figure 6A-B**), even in generations where flow sequencing is not prominent (**Figure 4A**), and hence does not contribute to phase III slope at the mouth.

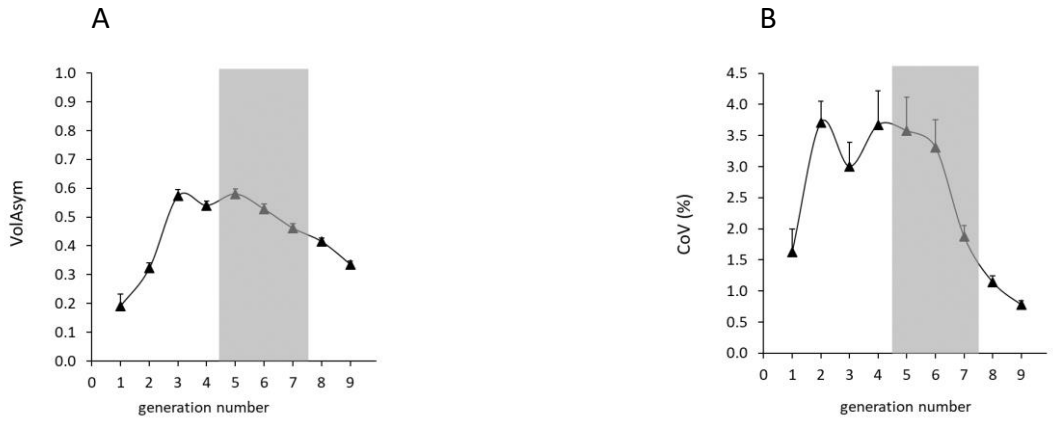

Figure 6: Generation-specific volume asymmetry (*VolAsym*) and concentration heterogeneity (CoV) as a function of airway generation number; same representation as Figure 4. Volume asymmetry and concentration heterogeneity do occur in generations proximal to generation 5, but in these proximal generations flow sequence does not contribute to a positive slope.

When considering flow sequencing and lung mechanical heterogeneity across all bronchial generations, there is a clear association of *seq[flow]* with compliance heterogeneity (rho=-0.61, p<0.001, Spearman Rank correlation) (**Figure 7A**), but not with resistance heterogeneity (p = 0.3), (**Figure 7B**). Of note, 49%, 40% and 11% of all the data points in **Figure 7** had respectively positive, almost no (between -0.5% and +0.5%), or negative *seq[flow]*.

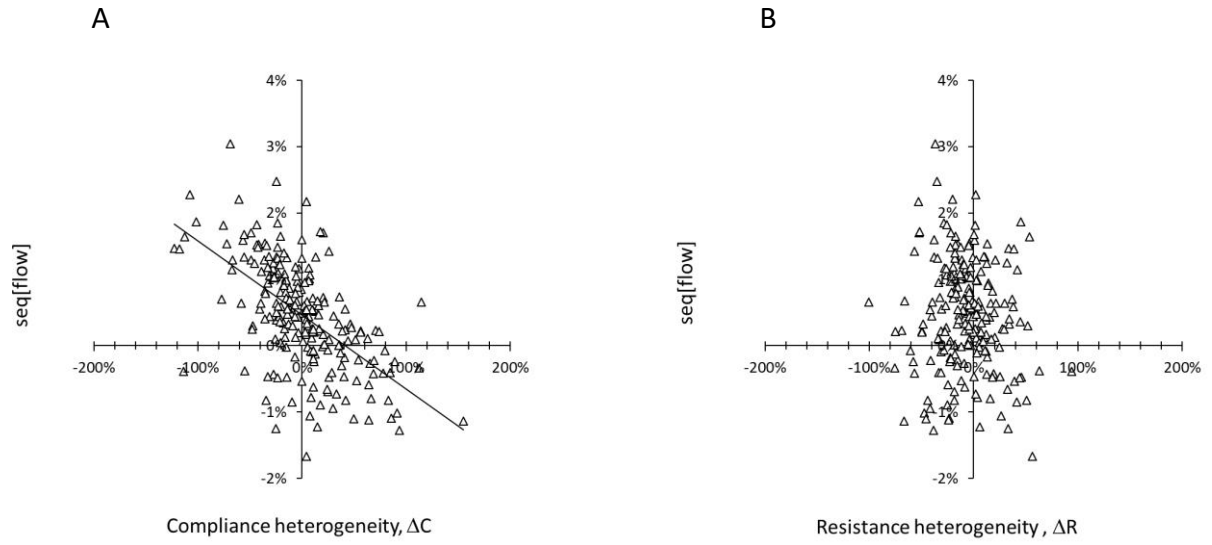

Figure 7: Generation-averaged flow sequencing (*seq[flow]*) versus corresponding heterogeneity of compliance (ΔC) (panel A) and heterogeneity of resistance (ΔR) (panel B) for all 24 lung structures. Flow sequencing is associated with degree of compliance heterogeneity but not with resistance heterogeneity. 49% of all data points have a markedly positive (> +0.5%) *seq[flow]*; instances of markedly negative (< -0.5%) *seq[flow]* (11%) are dominated by branchpoints with positive ΔC (4th quadrant).

To test for potential non-linear influences of local radius heterogeneity on flow sequencing, all simulations were repeated in the 24 structures by setting branch radii of each set of 2 daughter airways equal to their average radius, while preserving branch length. These simulations (**Figure 8**) also show positive flow sequencing in generation 5-7, as was the case in **Figure 4A**.

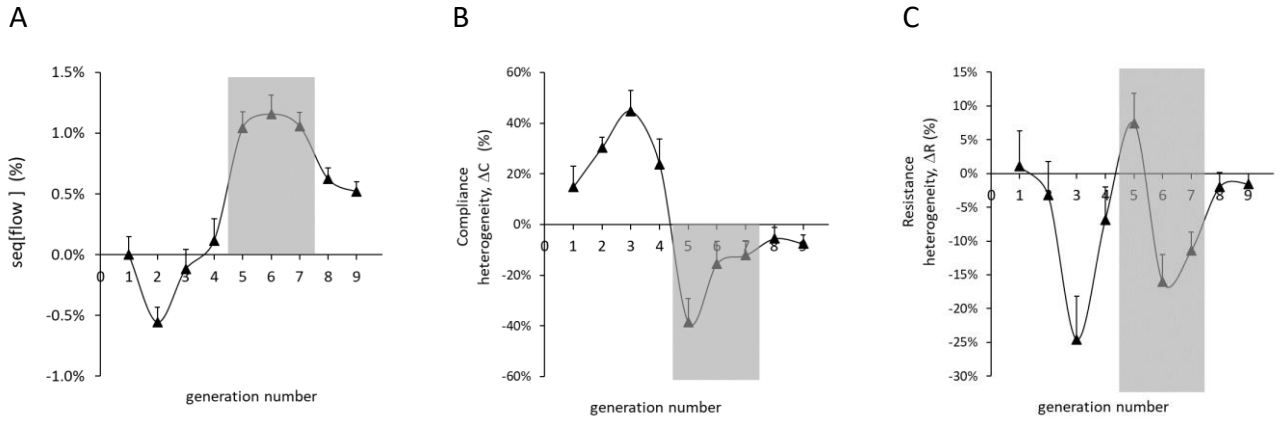

Figure 8: Generation-specific flow sequence, compliance heterogeneity and resistance heterogeneity as a function of airway generation number, after imposing radius homogeneity. Results in Figure 4 were recreated after setting the radius of each pair of daughter branches equal to their mean; same representation as Figure 4.

DISCUSSION

In this study, we have quantified the degree of flow sequencing that is responsible for generating phase III slopes, and thus contribute to ventilation heterogeneity measures (Scond) in asthmatic patients. We verified that average flow sequencing (*seq[flow]*) values peaked in generations 5-7 (**Figure 4**) such that any concentration difference arising in daughter generations 6-8 would be expected to translate into a phase III slope one generation downstream during exhalation. We then compared the *seq[flow]* to characteristics of the bronchial tree at individual branch points, demonstrating that compliance heterogeneity, as opposed to resistance heterogeneity, was the most prominent driver of flow sequencing (**Figures 4-7**). Compliance heterogeneity in these lung structures is mostly due to the asymmetrical distribution of the terminal units. Within the asthma literature there has been sustained focus on the role of the small airways in dysfunction, and the question of whether asthmatic pathophysiology is more dominantly driven by small or large airway morphology.[11,14] The present data shows that the bronchial asymmetry effectively induces a compliance heterogeneity at the level of mid-size conductive airways (generations 5-7 where it generates a major contribution to ventilation heterogeneity detected at the patient's mouth.

In a simple two-compartment model, one would expect the daughter branch (and its subtended volume unit) with the lower washout concentration to be automatically associated with the higher compliance (i.e., positive ΔC) or lower resistance (i.e., negative ΔR). A priori, one would also not suspect there to be any strong flow sequencing between these two units. This is indeed what we observe in generations 1-4. However, from generation 5 onwards the majority of *seq[flow]* values are seen to be positive in the bronchial trees we studied, across all generations and patients in most cases (**Figure 7**). There are also instances where individual branch points have very little positive flow sequencing, leading to an almost zero or negative phase III slope. However, the net effect across all combined serial and parallel branch points is a predominance of positive flow sequencing, resulting in a positive phase III slope at the mouth. From the overriding effect of positive flow sequencing, particularly in generation 5-7, and its link to compliance heterogeneity, we can identify the latter as the defining feature.

In our CT based models, compliance heterogeneity is linked to the asymmetrical arrangement of the terminal units dictated by the asymmetry in the CT visible part of the bronchial tree and by the lobar boundaries. Thus, while compliance heterogeneity is partly due to the volume asymmetry of the bronchial tree itself, the space-filling algorithm beyond the actual CT-visible branches also play a role. There are many ways to fill the virtual space, but it is unlikely that a different space-filling algorithm would have affected compliance heterogeneity significantly, as any reasonable algorithm would be similarly constrained by the lung lobar boundaries, and potential energy minimization requirements.[10] One could argue that if the asymmetry in the virtual part of the model had been measurable at all in these airway generations (essentially beyond generation 7), these might have contributed to flow sequencing and phase III slope as well. There are two arguments against this possibility. One is that any such additional phase III slope contribution would accumulate with the current simulated phase III slopes, and thus overshoot the experimental phase III slopes for which a quantitative agreement was obtained[6]. Second, flow sequencing appears to be determined by bronchial asymmetry (in terms of ΔHorsf, ΔV or ΔC) which shows a critical and consistent change in sign in the transition between generation 4 and 5. We suspect this is dictated by the lung boundaries and the available space for terminal units, and it is difficult to imagine how different a truncation pattern in the virtual arrangement of peripheral units would have to be, in order to significantly alter this.

We assumed that some relationship would exist between overall asymmetry of the subtended lung units (*VolAsym*) and concentration heterogeneity (*CoV(conc)*), and indeed a considerable degree of bronchial asymmetry exists in generations where concentration heterogeneity develops (**Figure 6**). However, a direct comparison is difficult for two reasons. Firstly, given that *VolAsym* was defined to be between 0 and 1, and to increase with degree of asymmetry, it is not possible to allocate preferential status to the airway with the lower washout concentration as was the case for heterogeneity of subtended volume, compliance and resistance (ΔV, ΔC, ΔR). Secondly, both *VolAsym* and *CoV(conc)* in proximal generations are not only determined by the local asymmetry and concentration, but also by the more peripheral lung units subtended by them. This means that isolation of effects at the individual branch level is difficult, due to these fractal-like dependencies. This contrasts with *seq[flow]*, which is

only determined by local flow rates into a given branch point (though flow rates themselves are dependent on subtended resistance and compliance).

We anticipated that unequal radii of two sister branches could have partly contributed to local flow sequencing. Yet the repeat simulations with identical radii for each pair of daughters showed very similar patterns to the ones with variable radii (**Figure 8**). However, we could not modify these structures to exclude the effects of local resistance heterogeneity altogether, as branch length also influences airflow resistance. Modifying a given virtual structure such that paired daughter radii are equal, is a trivial task. However, applying the same modifications to branch lengths requires completely restructuring a tree, as changing the spatial location of a branch terminus directly affects all subtended branches in a cascading effect, which could cause downstream branches to exceed the confines of the lobar boundaries. Given this, it would have been impossible to alter structure branch lengths to ensure homogeneity of daughter pairs, while adhering to the CT-derived lobe bounds, and maintaining the original compliance heterogeneity (which would be altered by removal of any branches). Since radius has a much greater impact on resistance than airway length, the added simulations with equal radii for both daughter airways was likely sufficient to show that bronchial trees of asthma patients with artificially reduced local resistance heterogeneity still produced positive flow sequencing in generations 5-7.

Present findings, where bronchial asymmetry is key, can also be linked to physiological measurements in normal subjects where bronchoprovocation has been seen to lead to several-fold increases in convection-dependent slopes (Scond)[15], and in asthmatic patients in whom Scond was identified as an independent predictor of hyperresponsiveness.[16] Our findings may also explain the link between MBW-based Scond and ventilation defects observed with SPECT.[17] Likely, the underlying common denominator is that a situation is created where bronchial occlusion occurs, generating dramatic changes in the asymmetry of the communicating compliant units, thus generating flow sequencing as illustrated in **Figure 2**. Our findings likely also pertain to physiological measurement of mechanical properties by intra-breath oscillometry[18] which could be partly driven by the within-breath

flow sequencing in a range of bronchial generations that we describe here. The connection between convective ventilation distribution and lung mechanics has already been studied by Gillis and Lutchen[19], who obtained a flow (ventilation) distribution in a bronchial network from a solution in the frequency-domain of a mechanical network model of histamine provocation. Extrapolated to intra-breath lung mechanics, a time-dependent solution of the mechanical network model could potentially reveal how exactly flow sequencing such as depicted in **Figure 2** emerges as a result of compliance heterogeneity, and why it does so specifically in mid-range conducting airway generations.

Study limitation

The models used here did not account for any heterogeneity in acinar compliances yet did account for gravitational variations in specific ventilation, through influence of local pleural pressure. We did not consider a sigmoid P-V curve which, together with the difference in gravity-dependent specific ventilation, would have induced large-scale ventilation heterogeneities with flow sequencing between top and bottom of the lungs. Scintigraphy data by Anthonisen[20] has suggested that such flow asynchrony could exist, associated with the shape of the P-V curve, but this is usually thought to pertain to vital capacity breaths. Alternatively, dynamic CT imaging of lobar expansion and contraction during normal breathing obtained in just 5 normal subjects[21] did hint at a degree of flow sequencing that could lead to a phase III slope, but this was heavily weighted by the right middle lobe.[22] Since the gravity-dependent portion of phase III slope during near-tidal breathing is expected to be small,[23] and the exact nature of flow sequencing between gravity-dependent lung units remains unknown, we have refrained from incorporating this specific aspect here. In any case, the range of phase III slopes in the asthma patients under study largely exceeds any potential contribution from gravity-dependent flow sequencing. Another aspect that could have modulated the outcome are dynamic airway changes, which were not incorporated in our patient bronchial models, which were based on inspiratory CT images and thus did not account for intra-breath airway changes. However, this work has shown that the predominant effect is that of bronchial asymmetry leading to the acinar units, eliciting dramatic changes in heterogeneity of effective compliance. Hence we suspect any dynamic change in the airways would only mildly have affected the general outcome, unless of course in cases of complete airway closure. Finally, we considered total breathing flow to be constant over inspiratory and expiratory

phases. Given the patterns of flow asynchrony that we obtained (exemplified in **Figure 2**) we suspect that the main message would not be affected much by for instance, a skewed breathing pattern with long tails at low breathing flow. To deal with this in a quantitatively meaningful way would require the incorporation of altered lung mechanical properties at these low flows.

CONCLUSION

Within this study we have used a validated model of pulmonary gas dynamics to quantify the morphologic features of the conducting zone which most strongly contributed to flow sequencing in asthmatic patients. Flow sequencing was seen to be consistently highest in generations 5-7 and was most strongly influenced by the underlying compliance heterogeneity of the lung – compliance heterogeneity itself being mostly influenced by asymmetrical distributions of subtended volume units. These results suggest that the aggregation of structural features of the small conducting airways through airflow patterns in mid-sized conducting airways may drive significant portions of ventilation heterogeneity in asthma.

REFERENCES

1. Verbanck S, Paiva M. Gas Mixing in the Airways and Airspaces. Comprehensive Physiology 2011;1(2):809–34.
2. Svenningsen S, Eddy RL, Lim HF, Cox PG, Nair P, Parraga G. Sputum eosinophilia and magnetic resonance imaging ventilation heterogeneity in severe asthma. American Journal of Respiratory and Critical Care Medicine 2018;197(7): 876-884
3. Hamedani H, Kadlecek S, Ruppert K, Xin Y, Duncan I, Rizi RR. Ventilation heterogeneity imaged by multibreath wash-ins of hyperpolarized 3He and 129Xe in healthy rabbits. The Journal of Physiology 2021;599(17):4197–223.
4. Farrow CE, Salome CM, Harris BE, et al. Airway closure on imaging relates to airway hyperresponsiveness and peripheral airway disease in asthma. https://doi.org/101152/japplphysiol016182011 2012;113(6):958–66.
5. Verbanck SAB, Polfliet M, Schuermans D, et al. Ventilation heterogeneity in smokers: role of unequal lung expansion and peripheral lung structure. https://doi.org/101152/japplphysiol001052020 2020;129(3):583–90.
6. Foy B, Kay D, Siddiqui S, Brightling C, Paiva M, Verbanck S. Increased ventilation heterogeneity in asthma can be attributed to proximal bronchioles. European Respiratory Journal. 2020; 55(3).
7. Foy BH, Gonem S, Brightling C, Siddiqui S, Kay D. Modelling the effect of gravity on inert-gas washout outputs. Physiological Reports. 2018; 6(10): e13709
8. Foy BH, Kay D. A computational comparison of the multiple-breath washout and forced oscillation technique as markers of bronchoconstriction. Respiratory Physiology and Neurobiology 2017; 270: 61-69
9. Foy BH, Kay D, Bordas R. Modelling responses of the inert-gas washout and MRI to bronchoconstriction. Respiratory Physiology and Neurobiology 2017; 235: 8-17
10. Bordas R, Lefevre C, Veeckmans B, et al. Development and analysis of patient-based complete conducting airways models. PLoS ONE 2015; 10(12): e0144105
11. Foy BH, Soares M, Bordas R, et al. Lung Computational Models and the Role of the Small Airways in Asthma. American Journal of Respiratory and Critical Care Medicine 2019; 200(8): 982-991
12. Gonem S, Berair R, Singapuri A, et al. Fevipiprant, a prostaglandin D2 receptor 2 antagonist, in patients with persistent eosinophilic asthma: a single-centre, randomised, double-blind, parallel-group, placebo-controlled trial. The Lancet Respiratory Medicine 2016; 4(9): 699-707
13. Pedley TJ, Schroter RC, Sudlow MF. The prediction of pressure drop and variation of resistance within the human bronchial airways. Respiration Physiology 1970;9(3):387–405.
14. Donovan GM, Noble PB. Small airways vs large airways in asthma: time for a new perspective. Journal of Applied Physiology 2021; 131(6): 1839-1841
15. Verbanck S, Schuermans D, Noppen M, Vincken W, Paiva M. Methacholine versus histamine: paradoxical response of spirometry and ventilation distribution. https://doi.org/101152/jappl20019162587 2001;91(6):2587–94.
16. Downie SR, Salome CM, Verbanck S, Thompson B, Berend N, King GG. Ventilation heterogeneity is a major determinant of airway hyperresponsiveness in asthma, independent of airway inflammation. Thorax 2007;62(8):684–9.
17. Rutting S, Chapman DG, Thamrin C, et al. Effect of combination inhaled therapy on ventilation distribution measured by SPECT/CT imaging in uncontrolled asthma. https://doi.org/101152/japplphysiol010682020 2021;131(2):621–9.
18. Gray DM, Czovek D, McMillan L, et al. Intra-breath measures of respiratory mechanics in healthy African infants detect risk of respiratory illness in early life. European Respiratory Journal 2019;53(2):1800998.
19. Gillis HL, Lutchen KR. How Heterogeneous Bronchoconstriction Affects Ventilation Distribution in Human Lungs: A Morphometric Model. Annals of Biomedical Engineering 1999 27:1 1999;27(1):14–22.
20. Anthonisen NR, Robertson PC, Ross WR. Gravity-dependent sequential emptying of lung regions. https://doi.org/101152/jappl1970285589 1970;28(5):589–95.
21. Jahani N, Choi S, Choi J, Iyer K, Hoffman EA, Lin C-L. Assessment of regional ventilation and deformation using 4D-CT imaging for healthy human lungs during tidal breathing. https://doi.org/101152/japplphysiol003392015 2015;119(10):1064–74.
22. Verbanck S, Paiva M. Could lobar flow sequencing account for convection-dependent ventilation heterogeneity in normal humans? https://doi.org/101152/japplphysiol010492015 2016;121(2):589–91.

23. Prisk GK, Guy HJ, Elliott AR, Paiva M, West JB. Ventilatory inhomogeneity determined from multiple-breath washouts during sustained microgravity on Spacelab SLS-1. https://doi.org/101152/jappl1995782597 1995;78(2):597–607.

FIGURE LEGENDS

Figure 1 : Generation-averaged coefficient of variation of washout gas concentration (*CoV(conc)*) and flow sequence (*seq[flow]*) between any parallel pair of lung units as a function of airway generation number for all 24 lung structures, stratified according to patients' overall Scond value at the mouth (open circles : below median Scond; closed circles : at or above median Scond). While a non-zero CoV is present in most generations, a consistently positive *seq[flow*] value only exists in generations 5-9.

Figure 2: Relative airflow profiles throughout inhalation and exhalation for each pair of daughters to parents at branch generations 4, 6, and 8, for a representative asthmatic lung structure. Movement back and forth along the identify line represents no asynchrony, while higher curvature indicates higher asynchrony. Considerable flow asynchrony is seen to develop in generation 6, and less so in two generations up or down.

Figure 3: Relative airflow profiles throughout inhalation and exhalation for each pair of daughters to parents, with flow sequence developing at branches 2 and 3, but not at the other more peripheral or proximal branch points where the subtended structures are symmetrical (branch 1, 5 or 6).

Figure 4: Generation-specific flow sequence (*seq[flow]*), heterogeneity of compliance (ΔC) and heterogeneity of resistance (ΔR) as a function of airway generation number; data obtained from all 24 lung structures is presented as means±SE; grey area indicates the generation range responsible for maximal phase-III slope contribution.[6] For a positive slope to occur at the mouth, *seq[flow]* needs to be positive; using the same convention that daughter branch d_1 is the one with the lower washout concentration, corresponding compliance and resistance heterogeneity (equations 1 and 2) are shown in the same representation.

Figure 5: Generation-specific heterogeneity of Horsfield order (*ΔHorsf*) and heterogeneity of subtended volume (*ΔV*) as a function of airway generation number; same representation as Figure 4.

Figure 6: Generation-specific volume asymmetry (*VolAsym*) and concentration heterogeneity (CoV) as a function of airway generation number; same representation as Figure 4. Volume asymmetry and concentration heterogeneity do occur in generations proximal to generation 5, but in these proximal generations flow sequence does not contribute to a positive slope.

Figure 7: Generation-averaged flow sequencing (*seq[flow]*) versus corresponding heterogeneity of compliance (ΔC) (panel A) and heterogeneity of resistance (ΔR) (panel B) for all 24 lung structures. Flow sequencing is associated with degree of compliance heterogeneity but not with resistance heterogeneity. 49% of all data points have a markedly positive (> +0.5%) *seq[flow]*; instances of markedly negative (< -0.5%) *seq[flow]* (11%) are dominated by branchpoints with positive ΔC (4^{th} quadrant).

Figure 8: Generation-specific flow sequence, compliance heterogeneity and resistance heterogeneity as a function of airway generation number, after imposing radius homogeneity. Results in Figure 4 were recreated after setting the radius of each pair of daughter branches equal to their mean; same representation as Figure 4.